High quality factor two dimensional GaN photonic crystal cavity membranes grown on silicon substrate

N. Vico Triviño,[a] G. Rossbach, U. Dharanipathy, J. Levrat, A. Castiglia, J.-F. Carlin, K. A. Atlasov,[b] R. Butté, R. Houdré, and N. Grandjean
Institute of Condensed Matter Physics, École Polytechnique Fédérale de Lausanne (EPFL), CH-1015 Lausanne, Switzerland

(Received 23 December 2011; accepted 24 January 2012; published online 14 February 2012)

We report on the achievement of freestanding GaN photonic crystal L7 nanocavities with embedded InGaN/GaN quantum wells grown by metal organic vapor phase epitaxy on Si (111). GaN was patterned by e-beam lithography, using a SiO_2 layer as a hard mask, and usual dry etching techniques. The membrane was released by underetching the Si (111) substrate. Micro-photoluminescence measurements performed at low temperature exhibit a quality factor as high as 5200 at ~420 nm, a value suitable to expand cavity quantum electrodynamics to the near UV and the visible range and to develop nanophotonic platforms for biofluorescence spectroscopy. © *2012 American Institute of Physics*. [doi:10.1063/1.3684630]

Beyond their impact on solid state lighting, GaN and related alloys are promising semiconducting materials for both devices (e.g., gas sensors or on-chip biophotonic devices) and fundamental research. Their high oscillator strength (typically ten times larger than in GaAs-based alloys), large exciton binding energy (~26 meV for bulk GaN), and efficient light emission properties from the UV to the green wavelength range make them particularly suitable for the investigation of light-matter coupling phenomena. Thus, polariton lasing has been achieved in GaN-based microcavities at room temperature (RT),[1] which is not possible with smaller bandgap III-V compounds. Furthermore, owing to its near-UV bandgap, GaN is transparent in the visible range, which makes it an ideal candidate for fluorescence-based nano and micro-opto-electro mechanical systems.[2,3]

In this context, the demonstration of photonic crystals (PhCs), whose interest relies among others on the ability to control the spontaneous emission rate,[4] designed for short wavelength operation is highly desirable. Indeed, PhCs offer manifold possibilities to tailor the light,[5,6] as they can be built from many different materials, with diverse designs in different dimensions, and use a wide variety of embedded active media such as quantum dots (QDs),[7] quantum wires,[8] or quantum wells (QWs).[9] Moreover, in high quality factor (Q) PhC cavity slabs with a small mode volume, which require both careful design and fabrication,[10] a strong enhancement of the Purcell factor is expected.[11] Despite all those advantages, the development of GaN-based PhCs only started a few years ago.[12–14] It is mainly due to technological difficulties. Indeed, the shorter operating wavelength of such GaN photonic structures compared with smaller bandgap semiconductors (like silicon or III-As compounds) make them much more sensitive to fabrication defects that enhance undesired light scattering and to radiation losses arising from the smaller refractive index contrast with air. Therefore, higher lithographic resolution and smoother etched surfaces are required. Noticeably, improved fabrication and processing techniques allowed fast progress in recent years[15] as illustrated, e.g., by the report of AlN PhC cavity membranes with a Q factor ~1800 relying on the conformal growth of AlN on pre-patterned Si substrates.[16] Note as well that lasing has been recently reported in GaN PhC slabs at RT.[17,18] However, achieving Q values exceeding a few thousands in III-nitrides is challenging, although promising results have already been obtained like a Q factor of 2400 for an AlN PhC slab grown on 6H-SiC (0001).[14] Consequently, features such as the signature of the strong coupling regime, already observed in GaAs-based PhCs employing either QDs or QWs as an active region,[6,19] remained elusive so far with III-nitride cavities.

In this letter, significant progress is reported with the achievement at low temperature (LT) of high Q factor (~5200) in L7-type nanocavities based on GaN PhC membranes with embedded InGaN QWs.

The fabrication process started with the growth of a multilayer structure by metal organic vapor phase epitaxy on Si (111) substrate. A 60 nm thick low temperature AlN buffer layer was first grown in order to prevent the formation of cracks and to reduce the dislocation density caused by the large lattice mismatch between Si and GaN. Then a GaN layer (167 nm thick) followed by a double InGaN/GaN QW layer sequence consisting of $In_{0.2}Ga_{0.8}N$ (3.5 nm)/GaN (7 nm)/$In_{0.2}Ga_{0.8}N$ (3 nm), and finally, GaN (21 nm) was grown (Fig. 1). Note that thick QWs are highly desirable for achieving high Q factors as the absorption is weak on the ground state due to the quantum confined Stark effect (QCSE), which induces a large Stokes shift.[20] After the growth, a 100 nm thick SiO_2 layer was deposited on top of the epitaxial structure. This layer provides a hard-mask during the PhC fabrication avoiding GaN surface damage and pattern degradation. A $10 \times 10\ \mu m^2$ surface with a triangular lattice (air-filling factor $r = 0.35a$, lattice constant $a = 155$ nm) and a defect formed by seven missing holes at the center (L7-type nanocavity) were written by e-beam lithography after resist spinning. The orientation of such cavity is along $[10\bar{1}0]$. The pattern was transferred to SiO_2 by

[a]Author to whom correspondence should be addressed. Electronic mail: noelia.vicotrivino@epfl.ch.
[b]Present address: OPTEC LLC, 197022 St. Petersburg, Russia.

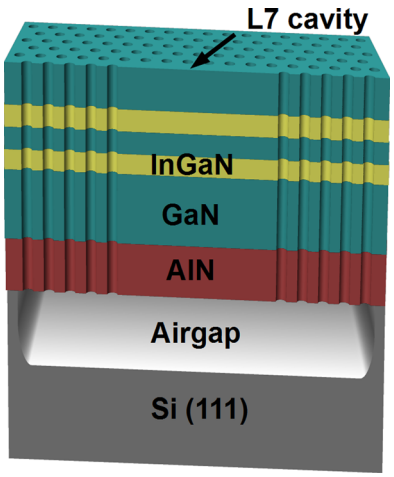

FIG. 1. (Color online) Schematic cross-section of a 2D GaN PhC L7 cavity with two embedded InGaN/GaN QWs.

reactive ion etching (RIE) and the resist was removed. Then GaN etching using chlorine-based inductively coupled plasma was carried out. Finally, the GaN membrane was released through dry RIE underetch of the Si (111) substrate.[21] An airgap of the order of 1 μm was achieved, which is large enough to minimize interactions with the substrate and related light losses. The SiO_2 mask was finally dissolved in a hydrofluorhydric acid solution.

Despite the processing complexity, two-dimensional (2D) GaN L7 PhC cavity slabs of high structural quality were obtained as shown in the scanning-electron-microscope (SEM) top and side views displayed in Figs. 2(a) and 2(b).

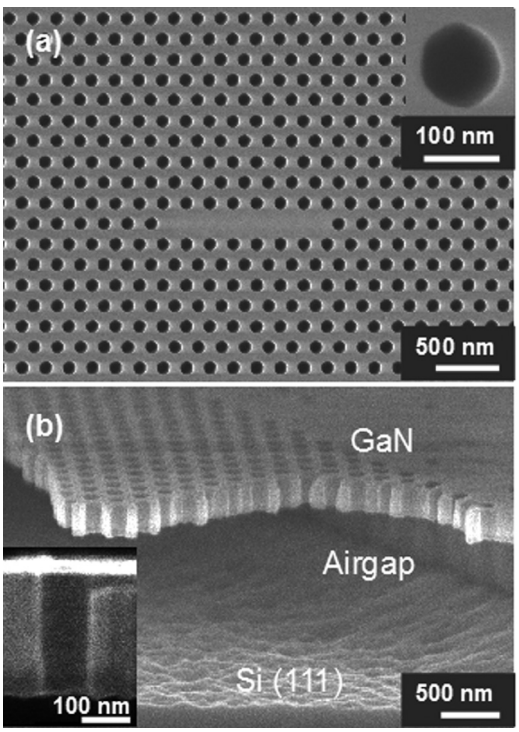

FIG. 2. (a) SEM top view of a L7 GaN cavity illustrating the high pattern regularity. Inset: Detail of one of the holes. (b) SEM side view (tilt of 15°) showing a large airgap (~1 μm). Inset: Single hole cross-section exhibiting a vertical and smooth profile.

We point out that the use of a SiO_2 hard mask seems to be determinant to ensure a low degradation of the pattern after completion of the whole process. The close-up view of one of the holes (inset of Fig. 2(a)) reveals a clear tendency toward a hexagonal shape due to the crystal structure, as already observed in similar AlN PhCs.[14] It is worth noticing that our cavities were not tuned by displacing adjacent cavity holes,[10] which is a widely used approach to further increase the Q factor. The large airgap achieved through substrate underetching is shown in Fig. 2(b). A hole cross-section is displayed in the inset exhibiting a vertical and smooth profile with a diameter ~100 nm.

Structures were characterized at LT by microphotoluminescence (μPL) spectroscopy using a continuous wave (cw) frequency-doubled Ar^+ laser ($\lambda = 244$ nm) focused down to a 2 μm diameter at an excitation power density of 2 kW/cm^2. The signal was then sent to a liquid-nitrogen cooled UV-enhanced charge-coupled device monochromator combination providing a spectral resolution of up to ~100 μeV. A typical μPL spectrum is shown in Fig. 3(a).

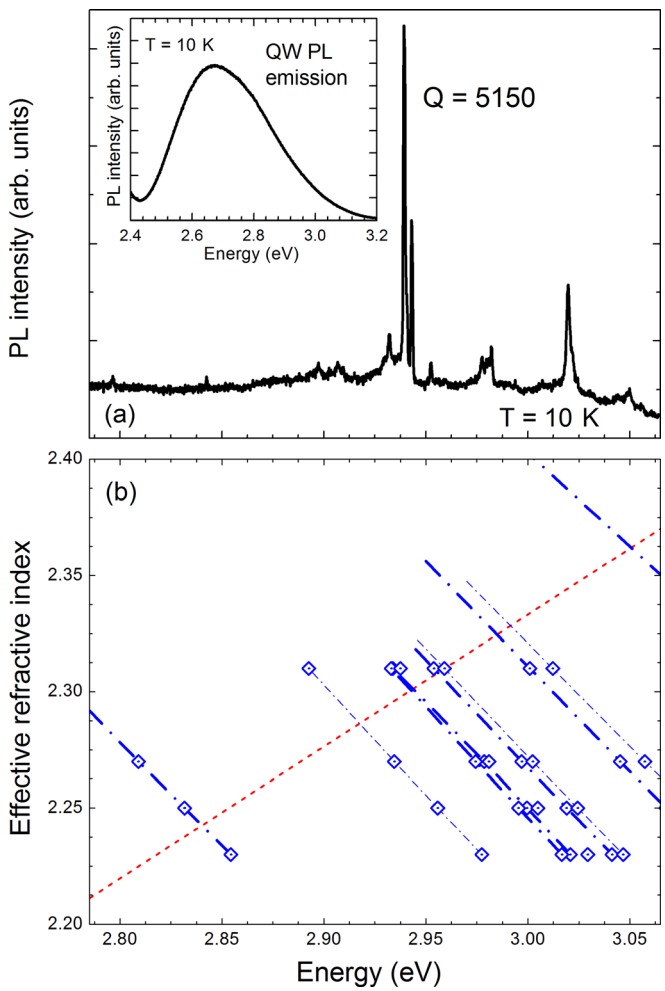

FIG. 3. (Color online) (a) μPL spectrum acquired at LT under non-resonant cw-excitation. Inset: LT QW PL spectrum taken out of the PhC zone. (b) Cavity mode positions calculated for a given n_{eff} value are represented by squares. Each blue dash-dotted line represents the spectral dispersion of the cavity modes issued from the TE1 guided mode, taking into account the dispersion of the effective refractive index (red dashed line), which is assumed to be linear in the spectral range of interest.

Six main peaks are distinguished at 2.932, 2.938, 2.942, 2.952, 2.980, and 3.02 eV. The narrowest one, emitting at 2.938 eV, has a linewidth of 570 μeV corresponding to a Q factor as high as 5150.

To analyze the experimental spectra, we use the 2D plane wave expansion method for the calculation of the photonic crystal dispersion and cavity modes.[22] The L7 PhC cavity induces multiple states inside the bandgap. Similar L7 multimode cavities were already studied in GaN membranes.[13] In addition, owing to the thickness of our waveguide, three orders of transverse electric (TE) and transverse magnetic (TM) modes are supported among which only the first two TE modes provide a bandgap in the PhC. At this stage, one should point out that to properly determine the mode eigenfrequencies the refractive index dispersion of GaN (Ref. 23) has to be accounted for. Only the AlN and GaN contributions were included for the estimation of the effective refractive index (n_{eff}) used in 2D calculations. The InGaN refractive index was disregarded due to the relative thin thickness (~6.5 nm) of QW layers compared to that of the whole structure (~240 nm). The estimated n_{eff} is displayed in Fig. 3(b) (red dashed line). The position of the cavity modes was then calculated for various n_{eff} values and is represented by squares in Fig. 3(b). This way the dispersion of each cavity mode (blue dash-dotted lines) is obtained. One can determine the dispersion-corrected mode positions from the intersections of the cavity mode dispersion (blue dash-dotted lines in Fig. 3(b)) and that of the effective refractive index dispersion (red dashed line). The mode positions resulting from these intersection points can then be directly compared with their position on the experimental spectrum shown in Fig. 3(a). Differences between the theoretical and experimental mode positions could be ascribed to discrepancies in the index dispersion between Ref. 23 and this work. They are expected as a consequence of several factors such as strain induced during growth on mismatched materials (AlN and Si) which is favored by our thin membrane thickness, or the etching of the substrate to release the membrane. We have also performed three-dimensional finite element and finite difference time domain simulations to validate the position of the main cavity modes and their field profile along with their Q factor. They are all found to be in reasonable agreement with the values extracted from μPL experiments. It is also worth noticing that apart from sample imperfections absorption has also to be taken into account since it could drastically decrease the Q factor. Indeed, the experimental Q^{-1} values depend among others on the absorption by means of the relationship $Q_{abs}^{-1} \propto \alpha\lambda$, where α is the mean absorption coefficient in the cavity arising from the GaN cavity and InGaN QWs. In our spectral region, absorption in GaN is expected to be quite low ($<30\,cm^{-1}$),[24] indicating that the limitation could arise from InGaN QWs. If the QW absorption is expected to be rather weak at the PL peak energy of ~2.7 eV (inset of Fig. 3) due to the QCSE, it is expected to increase at higher energy because of absorption by the excited states.[20] Thus, stronger absorption at higher energies is expected in such QWs. Similar trends were observed in microdisks with analogous active layers.[25]

In summary, a Q factor as high as ~5200 has been measured in 2D GaN PhC cavity slabs with embedded InGaN QWs emitting at ~420 nm. It is shown that an accurate description of the cavity modes needs to fully take into account the dispersion of the effective refractive index close to the GaN band gap. The present work should pave the way toward even larger Q factors in such nanocavities by shifting adjacent cavity holes,[10] increasing the QW emission further in the visible to minimize absorption, or exploiting less absorbing media such as QDs. It should also have direct consequences on the extension of cavity quantum electrodynamics to short wavelengths and high-temperature, including strong light-matter coupling phenomena, and on the development of integrated photonic circuits or micro-optofluidic devices for biophotonics.

The authors would like to thank P. Gallo and D. Zhaolu for fruitful discussions. This work was supported by the NCCR Quantum Photonics, research instrument of the Swiss National Science Foundation (SNSF) and by the SNSF (Grant No. 200020-113542).

[1]S. Christopoulos, G. B. H. von Högersthal, A. J. D. Grundy, P. G. Lagoudakis, A. V. Kavokin, J. J. Baumberg, G. Christmann, R. Butté, E. Feltin, J.-F. Carlin *et al.*, Phys. Rev. Lett. **98**, 126405 (2007).
[2]R. P. Tompkins, J. M. Dawson, L. A. Hornak, and T. H. Myers, Proc. SPIE **7056**, 70560J (2008).
[3]S. Yamada, B.-K. Song, T. Asano, and S. Noda, Appl. Phys. Lett. **99**, 201102 (2011).
[4]E. Yablonovich, Phys. Rev. Lett. **58**, 2059 (1987).
[5]S. Noda, M. Fujita, and T. Asano, Nature Photon. **1**, 449 (2007).
[6]M. Soljacic and J. D. Joannopoulos, Nature Mater. **3**, 211 (2004).
[7]T. Yoshie, A. Scherer, J. Hendrickson, G. Khitrova, H. M. Gibbs, G. Rupper, C. Ell, O. B. Shchekin, and D. G. Deppe, Nature (London) **432**, 200 (2004).
[8]K. Atlasov, K. F. Karlsson, E. Deichsel, A. Rudra, B. Dwir, and E. Kapon, Appl. Phys. Lett. **90**, 153107 (2007).
[9]M. Fujita, S. Takahashi, Y. Tanaka, T. Asano, and S. Noda, Science **308**, 1296 (2005).
[10]Y. Akahane, T. Asano, B.-S. Song, and S. Noda, Nature (London) **425**, 944 (2003).
[11]E. M. Purcell, Phys. Rev. **69**, 681 (1946).
[12]T. N. Oder, J. Shakya, J. Y. Lin, and H. X. Jiang, Appl. Phys. Lett. **83**, 1231 (2003).
[13]Y.-S. Choi, K. Hennessy, R. Sharma, E. Haberer, Y. Gao, S. P. DenBaars, S. Nakamura, and E. L. Hu, Appl. Phys. Lett. **87**, 243101 (2005).
[14]M. Arita, S. Ishida, S. Kako, S. Iwamoto, and Y. Arakawa, Appl. Phys. Lett. **91**, 051106 (2007).
[15]A. Z. Khokhar, K. Parsons, G. Hubbard, F. Rahman, D. S. Macintyre, C. Xiong, D. Massoubre, Z. Gong, N. P. Johnson, R. M. De La Rue *et al.*, Microelectron. Eng. **87**, 2200 (2010).
[16]D. Néel, S. Sergent, M. Mexis, D. Sam-Giao, T. Guillet, C. Brimont, T. Bretagnon, F. Semond, B. Gayral, S. David *et al.*, Appl. Phys. Lett. **98**, 261106 (2011).
[17]C.-H. Lin, J.-Y. Wang, C.-Y. Chen, K.-C. Shen, D.-M. Yeh, Y.-W. Kiang, and C. Yang, Nanotechnology **22**, 025201 (2011).
[18]D.-U. Kim, S. Kim, J. Lee, S.-R. Jeon, and H. Jeon, IEEE Photon. Technol. Lett. **23**, 1454 (2011).
[19]D. Bajoni, D. Gerace, M. Galli, J. Bloch, R. Braive, I. Sagnes, A. Miard, A. Lemaître, M. Patrini, and L. C. Andreani, Phys. Rev. B **80**, 201308(R) (2009).
[20]E. Berkowicz, D. Gershoni, G. Bahir, E. Lakin, D. Shilo, E. Zolotoyabko, A. C. Abare, S. P. Denbaars, and L. A. Coldren, Phys. Rev. B **61**, 10994 (2000).
[21]S. Sergent, PhD thesis, Université de Nice Sophia Antipolis, 2009.
[22]K. Sakoda, *Optical Properties of Photonic Crystals* (Springer, Berlin, 2005).
[23]N. Antoine-Vincent, F. Natali, M. Mihailovic, A. Vasson, and J. Leymarie, J. Appl. Phys. **93**, 5222 (2003).
[24]F. Omnès, N. Marenco, B. Beaumont, Ph. De Mierry, E. Monroy, F. Calle, and E. Muñoz, J. Appl. Phys. **86**, 5286 (1999).
[25]D. Simeonov, E. Feltin, A. Altoukhov, A. Castiglia, J.-F. Carlin, R. Butté, and N. Grandjean, Appl. Phys. Lett. **92**, 171102 (2008).